Modulation of laccase catalysed oxidations at the surface of magnetic nanoparticles

Lu Ren, Hongtao Ji, Karine Heuzé, Bruno Faure, Emilie Genin, Pierre Rousselot Pailley, Thierry Tron

1 Modulation of laccase catalysed oxidations at the surface of magnetic nanoparticles

2 Lu Ren,[a] Hongtao Ji,[b] Karine Heuzé,*[b] Bruno Faure,[a] Emilie Genin,[b] Pierre Rousselot Pailley[a] and Thierry Tron*[a]

3   a. Aix Marseille Université, Centrale Marseille, CNRS, iSm2 UMR7313, 13397 Marseille, France. Email : thierry.tron@univ-amu.fr.
4   b. Institut des Sciences Moléculaires, Université de Bordeaux, CNRS UMR5255, 33405 Talence cedex. Email : karine.heuze@u-bordeaux.fr
5

6 We explored the coupling of laccases to magnetic nanoparticles (MNPs) with different surface chemical coating. Two laccase variants offering two
7 opposite and precise orientations of the substrate oxidation site were immobilised onto core-shell MNPs presenting either aliphatic aldehyde,
8 aromatic aldehyde or azide functional groups at the particles surface. Oxidation capabilities of the six-resulting laccase-MNP hybrids were compared
9 on ABTS and coniferyl alcohol. Herein, we show that the original interfaces created differ substantially in their reactivities with an amplitude from 1
10 to > 4 folds depending on the nature of the substrate. Taking enzyme orientation into account in the design of surface modification represents a way
11 to introduce selectivity in laccase catalysed reactions.

12 **Keywords:** magnetic nano-particles; chemical coating; laccase orientation; oxidations

13 1-Introduction

14 The urgent requirement for a sustainable development of human society goes with environmental and economic issues
15 that boost the development of catalysis. Regarding the increasing demand for environmentally friendly catalysis,
16 biocatalysis is a blooming field. The catalyst (enzyme) itself is produced from readily available renewable resources, is
17 biodegradable and essentially non-hazardous and nontoxic.[1] Enzymes do work under mild conditions (in water, at room
18 temperature and atmospheric pressure), and generate little waste products. The sustainable development model displayed
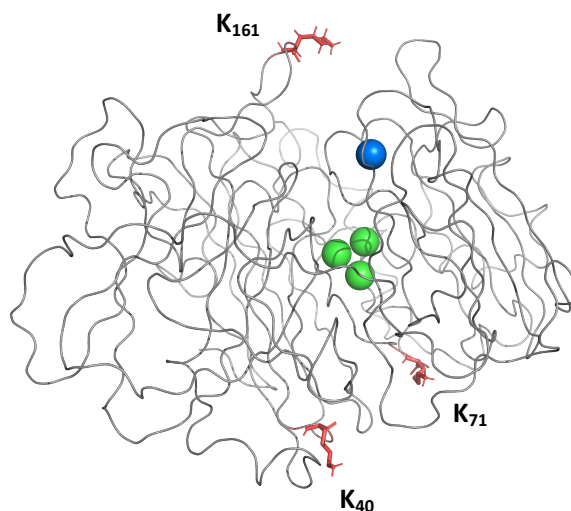19 by enzyme-catalysed processes fits perfectly what is pursued in the present century.

Figure 1: Model of the structure of the laccase LAC3 (Q6TH77) with three possible locations of lysine (side chain depicted in red) as they are present in the native enzyme (K_{71} and K_{40}) or in its UNIK$_{161}$ variant (K_{161}). Copper ions are depicted as colored spheres: blue (T1), green (TNC). View generated with PyMol (https://pymol.org/2/). Immobilization involving lysines of LAC3 will expose the T1 site to the solvent; immobilization involving the lysine of UniK$_{161}$ will expose the T1 site to the material surface. K is the one letter code for lysine (IUPAC amino acid code).

20 Laccases are multicopper enzymes.[2] They contain four copper ions distributed amongst two redox centres (Figure 1): a
21 surface located mononuclear T1 copper near which substrate oxidation occurs and a trinuclear cluster (TNC) formed from
22 a type 2 and type 3 copper ions, deeply embedded in the protein matrix where a four electrons reduction of molecular
23 oxygen takes place. Due to the presence of these copper ions in their catalytic centres, laccases have the distinctive ability
24 to couple the oxidation of a wide range of organic and inorganic compounds including substituted phenols (eq. 1), to the
25 production of harmless water (eq. 2). Robust enzymes, laccases are useful for diverse biotechnological applications, such

26 as bio bleaching in the textile industry, lignin degradation in paper production, bioremediation processes, organic synthesis
27 and for making bio-cathodes in biofuel cells.[3, , , 7]

$$4\ Ar\text{-}OH \longrightarrow 4\ Ar\text{-}O^{\bullet} + 4\ H^+ + 4e^- \quad (eq.1)$$

$$O_2 + 4\ H^+ + 4e^- \longrightarrow 2H_2O \quad (eq.2)$$

28 In order to meet industrial requirements efforts are made to make laccase even stronger and more robust biocatalysts.
29 Various cultivation techniques have been developed to efficiently produce laccase at the industrial scale.[8] Boosted yields
30 and simplified purification process in laccase production are now available due to the development of robust heterologous
31 expression systems.[9] Protein engineering offers the potential to tailor specific needs for efficient biocatalysts design.[10]
32 Besides, the use of redox mediators allows extending laccase substrate range from phenolic compounds to non-phenolic
33 compounds.[11] Additionally, immobilization of laccase on varieties of materials for different applications allows quick
34 separation and easy recycling.[12]

35 A main difficulty for an extensive use of laccases for organic synthesis remains their lack of selectivity. Indeed, the
36 mechanism by which these enzymes oxidize substrates is purely outer-sphere and does not require a properly defined
37 substrate binding site at the enzyme surface.[13, 14] Therefore, *in vitro*, radical species issued from mono-electronic substrate
38 oxidation (eq. 1) evolve independently of the enzyme. Molecular evolution techniques have been recently used to engineer
39 laccase towards chemo-selectivity with some encouraging success.[15] Besides, few attempts have been made to introduce
40 exogenously some selectivity in laccase catalysed reactions. For example, the laccase-TEMPO system is known for catalysing
41 the regio-selective oxidation of the primary hydroxyl groups of sugar derivatives, allowing polymer functionalization.[16]
42 Small organic cages like cyclodextrins have been shown to affect the fate of laccase mediated reactions.[17] To another
43 extend, it is known that switching from one solvent to another can have a great influence on the selectivity of reactions
44 catalysed by enzymes (substrate affinity, *ee*, regio and chemo selectivity).[18] In that direction, Danieli and coworkers
45 described for the first time a significant and unexpected influence of the solvent on the relative ratio of two dimers obtained
46 upon oxidative coupling of phenols catalysed by laccases.[19] Very recently, reports on bi-aryl coupling reactions suggest that
47 some fungal laccases could be remarkably selective *in vivo*, in particular through the help of accessory proteins acting
48 similarly to plant dirigent proteins (DIRs).[20]

49 Further to homogenous mixtures, exogenous materials brought close to the surface of enzymes during immobilization
50 processes are recognized to substantially affect enzymes' properties.[21] However, beyond a commonly accepted role in
51 improving enzymes' operational stability the interface between the protein, the material and the solvent is generally not
52 well known. Yet, partitioning and mass transfer effects surely tune enzyme kinetics, optimal operational pH, as well as
53 apparent substrate affinity and orientation. In the abundant literature devoted to laccase immobilizations, a control of the
54 enzyme's orientation is consistently pursued in the elaboration of bio-cathodes.[22] In this case it is the optimization of the
55 electron transfer which is pursued rather than reactivity at the surface of materials. As suggested by differences observed
56 in the enantio-selectivity of an immobilised lipase depending on the nature of the support,[23] altering the microenvironment
57 of a catalytic site at a material surface may represent a way to modulate enzymes selectivity. Taking enzyme orientation
58 into account in the design of surface modification represents a potential to introduce (and control) further selectivity in
59 laccase catalysed reactions.

60 Amongst all kinds of materials used for enzyme immobilization, superparamagnetic particles (MNPs) are one of the most
61 popular.[24] Besides the convenience of a separation based on the use of a simple magnet, MNPs combine a high specific
62 surface area and core-shell structures allowing to vary the reactive functional groups that cover the surface of the particles.
63 Such surface variations make it possible to choose not only the immobilization method but also the micro-environment of
64 the surface of the immobilised object. By playing both on the orientation of the enzyme during immobilization and on the
65 nature of the functionalization layer, a modulation of the selectivity may be expected.[25] Here, we report on the covalent
66 immobilization of a fungal laccase in two opposite orientations at the surface of core-shell MNPs offering three different
67 functionalization layers. It is shown that, when the enzyme's active site is not part of the interface, laccase activity remains constant
68 whatever the MNPs functional group is. To the contrary, varying MNPs surface chemical functions in the vicinity of the surface
69 accessible active site of laccase directly influence its activity and beyond its selectivity.

70 ## 2-Experimental

71 *2.1-Materials*

72 Unless otherwise stated, all chemicals and reagent used in the experiments were of analytical grade from commercial
73 source. All chemicals and TurboBeads® click were purchased from Sigma-Aldrich and used as received. BcMag™ Beads were

74 purchased from Bioclone Inc. (San Diego, USA). MNP2 beads were synthesized from core-shell γ-Fe₂O₃/SiO₂, 300 nm
75 superparamagnetic nanoparticles provided by Ademtech S.A, France (see below).

2.2-Custom synthesis of aldehyde activated particles (MNP2)
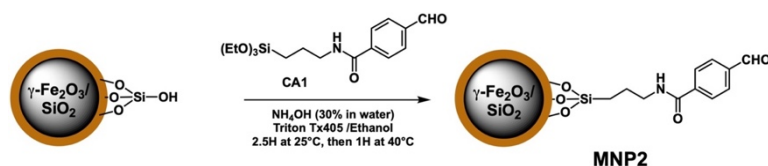
Scheme 1: Synthesis of MNP2

77 N-(3-triethoxysilylpropyl)-4-formyl benzamide (**CA1**) was synthesized according to Ahmadi et al.[26] To 10 mg of γ-Fe₂O₃/SiO₂
78 MNPs dispersed in a solution composed of 0.75 mL of 0.21 % Triton X-405 and 0.75 mL of ethanol a catalytic amount of 30
79 % NH₄OH (87 µL) was added. **CA1** (0.044 g, 0.125 mmol) dissolved in 0.5 mL of DMSO was then added dropwise over 2.5
80 hours to the suspension of particles under mechanical stirring (300 rpm) and under argon at 25°C. Afterwards, the
81 suspension was stirred for 1 hour at 40°C. Finally, the particles were separated by magnetic decantation from the reaction
82 medium, washed with 0.21 % Triton X-405 (5 × 1 mL) and stored at 4°C.
83 FT-IR analysis was performed on FT-IR Nicolet 6700 spectrometer equipped with DRIFT device (Fig. SI1). Custom made
84 MNP2 were further characterized by TEM. As evaluated from this analysis, the grafting of CA1 resulted in an increase of the
85 silica shell thickness of 6 nm compared to native particles (see Figure SI2 and Table SI1).

2.3-Physico-chemical characteristics of MNPs

87 MNPs characteristics are collected in Table 1. Density of grafts were determined by Fluorescence spectroscopy according
88 to Yan et al. [27] for MNP2.

Table 1: MNPs characteristics[a]

	MNP1	MNP2[b]	MNP3
Diameter (m)	$1000 \cdot 10^{-9}$	$300 \cdot 10^{-9}$	$50 \cdot 10^{-9}$
Specific area ($m^2 g^{-1}$)	≈ 100	≈ 11	≈ 15
Particles per mass unit (g^{-1})	$1.7 \cdot 10^{11}$	$4 \cdot 10^{13}$	$2 \cdot 10^{15}$ [d]
Density of graft (mol g^{-1})	$\approx 210 \cdot 10^{-6}$	$\approx 1900 \cdot 10^{-6}$	$\approx 100 \cdot 10^{-6}$
Linker length (Å)[c]	24.3-25.8	11.5-12.5	14.1-14.3

90 (a): data obtained from manufacturers except otherwise specified; (b): data
obtained in this study; (c): evaluated (calculation) from a simple model; (d)
91 calculated value

2.4-Measurement of zeta potential

93 Zeta Potential measurements were carried out on Horiba Scientific nanoparticle analyzer SZ-100. The measurements were
94 performed at 25°C for diluted aqueous suspension of MNPs at pH varying from 3.0 to 8.0 (Fig. SI3).

2.5-Laccases

96 The laccase LAC3 (from *Trametes* sp C30) and its variant UNIK₁₆₁ were produced in *Aspergillus niger* and purified as
97 previously described.[32] Laccase concentration was estimated by UV-visible spectroscopy (Cary 60, Agilent Technologies,
98 USA) using an $\varepsilon_{610 \, nm} = 5600 \, M^{-1} \cdot cm^{-1}$ for the T1 copper site. The molecular weight of the enzymes is MW≈ 80 000Da.

2.6-Enzyme immobilizations

100 Prior immobilization the storage buffer (20 mM phosphate buffer pH 6) was exchanged for the reaction buffer by
101 concentration-dilution through a 30 kDa VIVASPIN 2 device (Sartorius Stedim Biotech, Germany) with 5~6 times repeat of
102 centrifugation at 3000rpm 4°C. Magnetic particles were washed 3 times with Milli Q® water then suspended into the
103 reaction buffer by vortexing vigorously for 1-2 minute (Aldehyde particles) or bathing in an ultrasonic bath for 20 min (Azide
104 particles).

2.6.1-Immobilization to aldehyde particles

106 The procedure is adapted from the original procedure from MacFarland and Francis, 2005.[28] 2mg/mL magnetic particles,
107 the appropriate amount of laccase (500 and $100 \cdot 10^{-6}$ M final concentration respectively for MNP1 and MNP2) and 10 equiv.
108 (relative to the enzyme concentration) of Iridium catalyst were mixed in a final volume of 200µL of Reductive Amination
109 Buffer ($50 \cdot 10^{-3}$ M phosphate with 0.1 M sodium formate, pH 7.4) and incubated overnight at room temperature in a mixer
110 (Eppendorf, Germany) with a continuous rotation (1000 rpm). The resulting laccase immobilised-MNPs were then obtained

111   by repeated cycles of washing and magnetic separation (controlling each time activity in the wash solution) and stored in

112   Storage Buffer (0.1 M acetate buffer pH=5.7) at 4°C until use. The evolution of the immobilised laccase activity as function

113   of the initial laccase concentration is given Figure 2 in the main text.

114   *2.6.2-Immobilization to azide particles*

115     $50 \ 10^{-6}$ M (final concentration) of the appropriate laccase, 10 equiv. of 4-ethynylbenzaldehyde and Ir catalysts relative to the laccase

116   concentration were mixed in a final volume of 2.5 mL Reductive Amination Buffer ($50 \ 10^{-3}$ M aqueous phosphate with 0.1M sodium

117   formate, pH 7.4) and slowly stirred under magnetic stirring for 72 hours at room temperature. After reaction, the resulting alkynylated

118   enzymes were recovered by passing through a PD MiniTrap G-25 columns (Sigma Aldrich, France) and concentrated by ultrafiltration

119   using a 30kD VIVASPIN 2 device (Sartorius Stedim Biotech, Germany).

120   Then, 10mg/mL azide particles, $1 \ 10^{-6}$ M of alkynylated enzyme and 30 equiv. (relative to laccase concentration) of $CuSO_4$/Ascorbic

121   acid/ bathophenanthrolinedisulfonic solutions were mixed in a final volume of Click buffer ($50 \ 10^{-3}$ M Phosphate buffer pH=7.5). The

122   mixture was stirred overnight at room temperature in a mixer (1000rpm/min). After reaction, particles were magnetically separated

123   and the supernatant discarded. Particles were repeatedly washed/magnetically separated (controlling each time activity in the wash

124   solution) and stored in Storage Buffer (0.1M acetate buffer pH=5.7) at 4°C until use. The evolution of the immobilised laccase activity

125   as function of the initial laccase concentration is given Figure SI4.

126   *2.7-Enzyme loading evaluation (Elisa)*

127   The detailed procedure can be found in Zhou et al., 2018;[29] the entire process of ELISA employed in this study is depicted

128   Figure SI5.

129   Coating buffer: 0.2 M sodium carbonate/bicarbonate, pH 9.4; Washing buffer: 0.1 M phosphate, 0.15 M sodium chloride,

130   pH 7.2 containing 0.05% Tween 20; Blocking buffer: 2% (w/v) Bovine Serum Albumin (BSA) in Washing Buffer; Substrate

131   solution: 1 tablet of PNPP (Sigma S0942) dissolve into 10 mL Glycine buffer (0.1 M glycine, pH 10.4, with $1 \ 10^{-3}$ M $MgCl_2$ and

132     $1 \ 10^{-3}$ M $ZnCl_2$).

133   Briefly, standard enzyme samples with different concentrations and the immobilised enzyme samples were added to a

134   microplate, in a final volume of 100 µL in each well; the microplate was then covered and incubated at room temperature

135   for 2 hours or at 4 °C overnight. Supernatants were removed (the microplate was held on a magnetic stand when discarding

136   the supernatant) and the wells washed 3 times with 200 µL of washing buffer. Subsequently, blocking buffer (300 µL) was

137   added to each well and the microplate was then covered and incubated under agitation at 600rpm for 1 hour at room

138   temperature. After disposal of the blocking buffer (with the help of the magnetic stand), 100 µL of the biotinylated detection

139   AC (anti LAC3, 5000× dilution with blocking buffer) was added per well and the microplate was covered and incubated

140   under agitation at 600rpm for 1 hour at room temperature. Supernatants were discarded and the wells washed 5 times

141   with 200µL of washing buffer. Next, 100 µL of the enzyme conjugate Alkaline Phosphatase-streptavidin (1000× dilutions

142   with washing buffer) was added to each well and the covered microplate further incubated under agitation at 600rpm for

143   1 hour at room temperature. Supernatants were again discarded and the well washed 7 times with washing buffer.

144   Eventually, 100 µL of substrate (PNPP) solution was added to each well and the plate was incubated at RT until color

145   developed. Absorbance of PNP was read at 405nm with a plate reader. Standard curves based on measured absorbance

146   values were established allowing to calculate enzyme loadings (Fig. SI6).

147   *2.8-Theoretical evaluation of enzyme loads*

148   Efficiency of grafting depends on the MNP's specific area, on the number of function available for grafting and on the

149   efficiency of the coupling reaction. The following calculations are given to provide theoretical numbers (maxima) to

150   compare with experimental values of enzyme grafting. Data on MNPs are taken from Table 1. Projection of the enzyme (Ø

151     $\approx 4 - 5$nm) on a surface: $\pi r^2 = 1.3 - 2 \ 10^{-17}$ m^2; $\mathcal{A} = 6.023 \ 10^{23}$ mol^{-1} (Avogadro number).

152   <u>MNP1</u>: (100 m^2 g^{-1} / $1.3 - 2 \ 10^{-17}$ m^2 / $\mathcal{A}$) $\approx 8 - 13 \ 10^{-6}$ mol g^{-1}

153   Note: taking into account the specific area and the number of particles per mass unit given Table 1 the bead's surface is

154   calculated to be: $100 / 1.7 \ 10^{11} = 5.9 \ 10^{-10}$ m^2. This value appears surprisingly high for 1000 nm beads with a smooth surface

155   ($4\pi r^2 = 3.14 10^{-12}$ m^2) suggesting a rough silica shell greatly extending the surface available to grafting.

156   <u>MNP2</u>: (11 m^2 g^{-1} / $1.3 - 2 \ 10^{-17}$ m^2 / $\mathcal{A}$) $\approx 1 - 1.5 \ 10^{-6}$ mol g^{-1}

157   <u>MNP3</u>: (15 m^2 g^{-1} / $1.3 - 2 \ 10^{-17}$ m^2 / $\mathcal{A}$) $\approx 1.2 - 2 \ 10^{-6}$ mol g^{-1}

158   *2.9-Laccase activity measurements*

159   *2.9.1-ABTS oxidation*

160   The mono-electronic oxidation of ABTS results in the formation of a stable emerald green radical cation (ABTS$^{+\bullet}$).

161   Activities of the free and immobilised laccase were determined against 2,2'-azino-bis (3-ethylbenzthiazoline-6-sulphonic

162   acid) (ABTS) in 0.1 M of Acetate buffer pH 5.5 at 30°C. Formation of the cation ($\varepsilon_{420 \ nm} = 36000$ M^{-1}·cm^{-1}, calculation factor

163   27.8) was followed for 2 min using a spectrophotometer (Cary 60, Agilent Technologies, USA).

164 For the measurement of the free laccase activity, 10 µL of the appropriately diluted enzyme samples was added into 890
165 µL of 0.1 M of Acetate buffer pH 5.5 at 30°C; the enzymatic reaction was started by adding 100 µL ABTS solutions (50 10^{-3}
166 M) into the reaction mixture. For the determination of the immobilised laccase activity, the reaction contained 10 µL of
167 MNP-immobilised laccase suspension (20 µg of particles at 2 mg/ml concentration), 890 µL of 0.1 M Acetate buffer pH 5.5
168 (pre-heated to 30°C in a water bath), and 100 µL ABTS solutions (50 10^{-3} M). The amount of laccase oxidizing one micromole
169 of substrate per minute is defined as one unit (U). All the experiments were carried out as triplicates and all results
170 presented are average of triplicates.

171 *2.9.1-Coniferyl alcohol oxidation*
172 Laccases oxidize coniferyl alcohol generating a resonance stabilized 4-vinylphenoxyl radical (CA$^\bullet$) which dimerises (random
173 coupling) to form the (±) pinoresinol (PINO), (±) dehydrodiconiferyl alcohol (DHCA) and (±) erytro/threo guiacylglycerol
174 (GUA) dimers (Scheme SI1). Oxidations of coniferyl alcohol (CA) catalysed by free and immobilised laccase were carried out
175 in a 2 ml centrifuge tubes. All experiments were performed in 0.1 M acetate buffer, pH 5,5. The final concentration of CA
176 was 1.6mM; the amount of laccase used was variable depending on the experiment (generally 1U/L as measured with
177 ABTS). A thermomixer set at 30 °C and 1000 rpm was used for the incubation. Samples were taken out at given time points
178 and the reaction was stopped by addition of 1 volume of an acetonitrile solution of benzophenone (benzo: internal
179 reference for HPLC). For the immobilised laccase samples, particles were captured with a magnet prior injection onto the
180 HPLC column for analysis. HPLC analysis were carried out with a JASCO LC-4000 series HPLC (JASCO, Japan). Samples were
181 separated on a reverse phase Nucleosil 100-5 C18 column (Macherey-Nagel, Germany) with a mobile phase composed of
182 a mixture of water - acetic acid 3% (solvent A) and acetonitrile (solvent B) with the following gradient: 90% A 10 % B for 5
183 min then 10% solvent B to 50% in 20 min then plateau 50% solvent B for 2 min then back to 10% solvent B for 2 min (Fig.
184 SI7).

Results and discussion

Design of the laccase/MNP interface.

187 Demonstrations of targeted orientations of a fungal laccase at a material surface have been previously obtained for example
188 on functionalized carbon nanotubes.[30] LAC3 from *Trametes* sp. C30 is a typical fungal laccase produced in high yield as a
189 recombinant enzyme.[31] Its sequence contains naturally only two lysines, K_{40} and K_{71}, out of 501 residues. LAC3 is our
190 reference enzyme for the creation of variants, called UNIKs, with a unique surface accessible lysine residue.[32] Here, we
191 selected UniK$_{161}$ (K_{40}->M, K_{71}->H, R_{161}->K) the unique lysine side-chain of which is offering a single free reactive -NH$_2$ group
192 for a functionalization nearby the T1 copper site while the two natural free -NH$_2$ groups of LAC3 are offering the potential
193 of a dual surface functionalization diametrically opposed to the T1 copper site with respect to the TNC (Figure 1). These
194 laccase variants can be efficiently functionalized via a reductive alkylation of their discrete lysine groups in a reaction
195 adapted from Mc Farland and Francis.[33] Neither the surface mutations (K_{40}->M, K_{71}->H, R_{161}->K) nor a subsequent lysine
196 functionalization lead to a significant modification of the catalytic efficiency of enzymes.[30, 32]
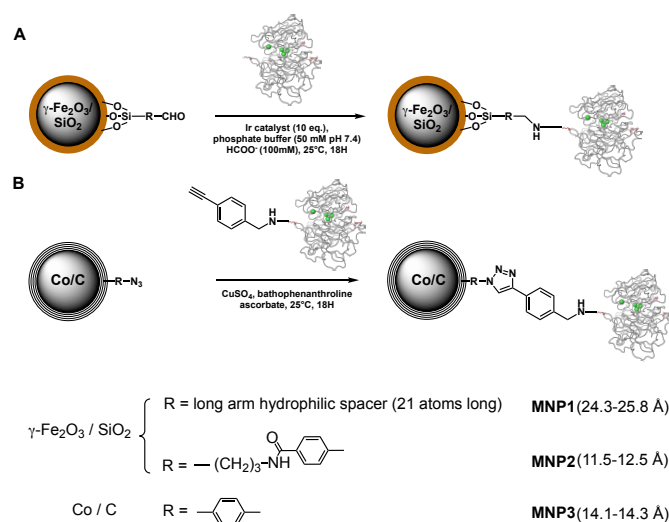
Scheme 2: Grafted core-shell MNPs. A: reductive alkylation; iron-oxide core/silica shell aldehyde particles; MNP1 = long arm hydrophilic spacer, MNP2 = aromatic spacer. B: azide-alkyne cycloaddition; cobalt core/carbon layers shell azido particles (MNP3); alkyne activated laccase (reductive alkylation). Approximative lengths of linkers (enzyme-to-shell) are given in brackets.

197 In order to modulate the physicochemical properties of the interface, MNPs with different surface functional groups were
198 selected for a covalent immobilization of the two laccase variants. Given the reactivity of the enzyme's lysine groups,
199 aldehyde-activated MNPs were targeted in the first place (Scheme 2A). Hence, the BcMag™ Beads from Bioclone that are
200 functionalized with an aldehyde group ending a long hydrophilic spacer (MNP1) and custom benzaldehyde activated γ-
201 Fe_2O_3/SiO_2 particles. On the other hand, providing a surface lysine is first activated with an alkyne (or azide) group, laccase
202 enzymes can be engaged in an alkyne-azide *Huisgen* 1,3-dipolar cycloaddition with no significant loss of activity.[30]
203 Therefore, TurboBeads® click (MNP3) were chosen for the immobilization of variants via click chemistry (scheme 2B). For
204 each MNP, the pH dependency of the zeta potential was evaluated from aqueous suspensions (Fig. SI3). Physicochemical
205 characteristics of the chosen MNPs are given in Table 1.

206 For both the reductive alkylation and the cycloaddition the selectivity of the functionalization reaction prevents the reaction
207 of non-lysine groups present on the protein surface with particles. After functionalization, particles were extensively
208 washed with a buffered solution to remove non-covalently bound enzymes. The resulting six different laccase/MNPs
209 hybrids were then compared for their ability to oxidize two different substrates, i.e. the synthetic substrate ABTS (2, 2'-
210 azinobis (3-ethylbenzothiazoline-6-sulfonic acid) and the natural substrate coniferyl alcohol (3-(4-Hydroxy-3-
211 methoxyphenyl)-2-propen-1-ol). Rather different in their structures (Scheme 3) these laccases substrates are proposed to
212 interact with different areas at the enzyme surface.[34]
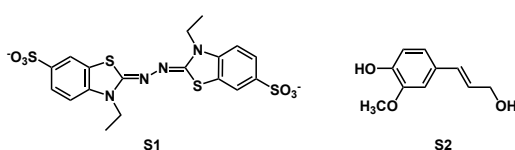
Scheme 3: Laccase substrates. **S1**: ABTS (2, 2'-azinobis (3-ethylbenzothiazoline-6-sulfonic acid); **S2**: coniferyl alcohol (3-(4-Hydroxy-3-methoxyphenyl)-2-propen-1-ol).

213 Determination of initial laccase concentration for the oriented immobilization of laccase

214 The immobilization process was studied using LAC3 as a model enzyme. Evolution of the immobilised laccase activity (ABTS
215 as substrate) as function of the initial laccase concentration used in the immobilization process is given Figure 2 for MNP1
216 and MNP2. As previously reported for other laccase-MNP hybrids,[35] for both particles, the activity of the immobilised
217 laccase increased linearly with the initial laccase concentration before reaching a plateau here from respectively 500 10^{-6}
218 M of enzyme for MNP1 and 100 10^{-6} M for MNP2. For MNP3 this plateau is reached at much lower concentration (10^{-6} M),
219 so the initial laccase concentration used was ranging from 1 to 10 10^{-6} M (Fig. SI4). A plateau is usually interpreted as a
220 "saturation", that could here apply either to the grafts or to the surface of the particles. Therefore, in subsequent
221 immobilization experiments initial laccase concentration was set to the value at which a plateau is reached, i.e. 100 10^{-6} M
222 for MNP1, 500 10^{-6} M for MNP2 and 10^{-6} M for MNP3.

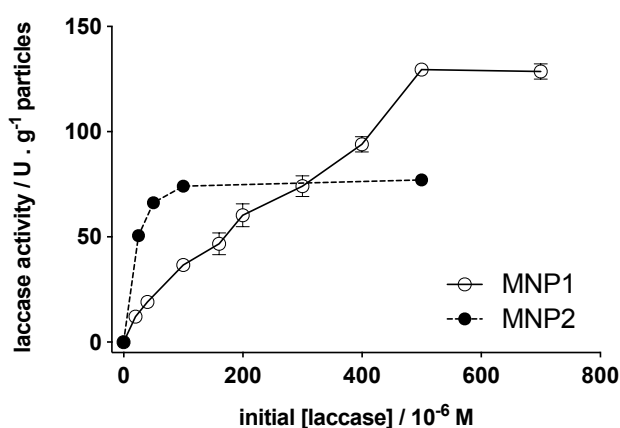**Figure 2:** Initial laccase concentration *versus* immobilised laccase activity. MNP1 and MNP2 particles concentration 2 g.L^{-1} incubated at 30°C in 0.1 M acetate buffer pH 5.5 in the presence of ABTS (5 10^{-3} M final). Kinetics of the radical cation formation followed spectrophotometrically at 420 nm (ε= 36 000 mol^{-1} cm^{-1}) for 2 min.

223 Hybrids activities appear consistent with results reported in literature.[36] However, multilayers or clusters of enzyme
224 molecules resulting from protein-protein interaction at the surface of the support may occur.[37] When enzyme molecules

225 are densely packed in multi-layers mass-transfer limitation results in a reduction of the activity of the immobilised
226 enzymes.[38] Then, consequences of the orientation of laccase on particles surface on its activity could be blurred. Therefore,
227 to be able to compare the effect of oriented immobilization on laccase activity, the concentration contributing to the
228 maximum activity of immobilised laccase should be determined first to reduce the influence of high density or multilayer
229 coverage at the greatest extent.

Enzyme loading

231 Enzyme loading is usually evaluated from a comparison of the concentration of proteins in solution before and after
232 immobilization. In the case of laccase, besides classical spectrophotometric (A_{280}) or indirect colorimetric (e.g. Bradford)
233 assays, an intense Cys(S)$\Rightarrow$Cu^{II} charge transfer band in the absorption spectrum of the oxidized enzyme ($\varepsilon \approx$ 5000-6000 M^{-}
234 ^{1} cm^{-1} at about 600 nm) can be used to determine the concentration. However, none of these assays were found practical
235 here principally because working with diluted solutions, protein concentrations are close to detection limits. Therefore, we
236 rather used an Enzyme Linked Immuno Sorbent Assay (ELISA) to quantify the amount of enzyme grafted onto MNPs (see
237 detailed procedure in SI). Commonly used for free proteins, ELISA may not be that frequently used for immobilised enzymes
238 quantification. It is then worth going through some experimental details to highlight its appropriateness in this case.

239 In this assay, LAC3-MNPs (antigens) first adsorbed to the wells of a microplate are complexed by a biotinylated anti-LAC3
240 antibody and tagged with a streptavidin-alkaline phosphatase for ultimate detection (Fig. SI5). The colorimetric titration of
241 product formation typically corresponds to a detection level in the range of picogram of antigen per well. Three
242 independent immobilizations of LAC3 and UniK$_{161}$ performed on each MNP were tested to evaluate enzyme loadings.
243 Freshly produced UniK$_{161}$ was used as standard enzyme for establishing calibration curves. For each measurement, two
244 different amounts of grafted MNPs were evaluated and the corresponding amounts of bare particles used as blank controls.
245 Standard samples and grafted MNP samples were tested in triplicate in a microwell plate. Curves depicting the relationship
246 between the absorbance of the end product at 405nm and the concentration of protein are shown in Figure SI6. Sampled
247 MNPs are within the working range of the curves. Product formation increases proportionally with the increase of particle
248 amount. As bare particles have no absorbance themselves (i.e. residual absorbance equivalent to that of the protein blank)
249 this increase in product formation correlates with amounts of immobilised enzymes in the well. Averaged enzyme loadings
250 are given Table 2.

Table 2. Amounts of enzyme grafted on the different MNPs (enzyme loading). Each value represents the mean of triplicates for two different amounts of particles.

	MNP1 (10^{-3}g/g)		MNP2 (10^{-3}g/g)		MNP3 (10^{-3}g/g)	
	LAC3	UNIK$_{161}$	LAC3	UNIK$_{161}$	LAC3	UNIK$_{161}$
I1	150	174	89	89	1.4	1.7
I2	187	165	92	90	2.5	2.4
I3	132	129	87	102	2.1	1.4

251 For each MNP, deviations observed for the three independent immobilizations (I1, I2, I3) are relatively small considering
252 the nature of the materials. Relative to each other, loads achieved are comparable for MNP1 and MNP2 and 1 to 2 orders
253 of magnitude lower for MNP3. Efficiency of enzyme immobilization depends on the MNP's specific area, on the number of
254 function available for grafting and on the efficiency of the coupling reaction. In view of their respective physicochemical
255 properties (Table 1), data from Table 2 highlight differences of grafting efficiencies for each MNP. Comparing experimental
256 values to an estimate of the maximum theoretical occupancy per particle unit (obtained relating the projected area of the
257 enzyme to the surface of the particle, see Experimental section for calculations), grafting efficiencies are evaluated to be
258 15 –25 %, 80 – 100 % and 1 – 2 % respectively for MNP1, MNP2 and MNP3(using a Mw≈80 000 Da for the enzymes). For
259 MNP2, the efficiency of the reductive alkylation reaction appears maximum and this correlates well with the saturation
260 observed earlier when varying the enzyme concentration (*vide supra*). On the other hand, for MNP1 the efficiency of the
261 coupling reaction is much lower and that despite MNP1 and MNP2 were grafted in the very same conditions. With an
262 amount two orders of magnitude higher than the estimated amount of grafted enzyme, availability of aldehyde group at
263 the surface of the MNP1 particles is not a limiting factor. Therefore, the relative decrease in efficiency of the coupling
264 reaction observed for MNP1 may be principally related to a lower reactivity of aliphatic aldehyde groups compared to
265 aromatic ones. Compared to the Cu promoted click reaction the reductive alkylation appears however particularly efficient.
266 Anyway, whatever the functionalization mode, it is noteworthy that enzyme orientation does not seem to influence the
267 grafting efficiency. This pre-requisite verified, activities of MNPs with opposite orientations of enzymes were then
268 compared.

Activity of immobilised laccases

270 **Oxidation of ABTS.** The mono-electronic oxidation of ABTS results in the formation of a stable emerald green radical cation (ABTS$^{\bullet+}$).
271 The kinetic of ABTS oxidation was followed in stirred solutions containing either a free laccase (LAC3 or UniK$_{161}$) or a laccase-MNP
272 hybrid (2 g.L^{-1}) derived from three independent immobilizations of LAC3 and UniK$_{161}$ performed on each MNP. For each
273 immobilization, free LAC3 or UniK$_{161}$ activity per milligram of total protein, i. e. their specific activity (SA), was similar (from 70 to 170
274 U.mg^{-1} depending on batches). SA of the different batches of laccase-MNP hybrids is compared Figure 3.
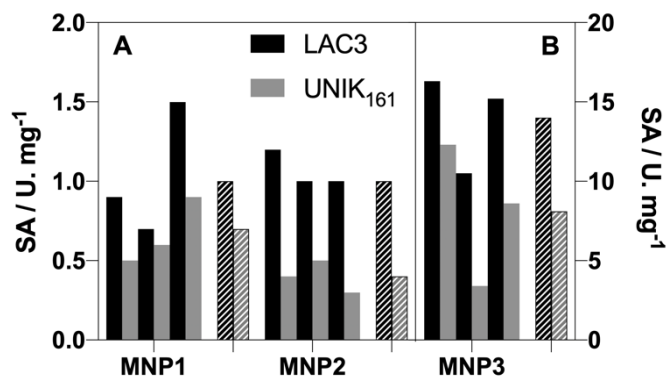

Figure 3: Specific activity of laccase-MNP hybrids towards ABTS. For each MNP, comparison of three sets of particles (I1 to I3 from Table 2) independently grafted either with LAC3 or UniK$_{161}$. A: aldehyde functionalized particles; B: azide functionalized particles. Laccase-MNP hybrids (2 g.L^{-1}) incubated at 30°C in 0.1 M acetate buffer pH 5.5 in the presence of ABTS (5 mM final). Kinetics of the radical cation formation followed spectrophotometrically at 420 nm (ε= 36 000 mol^{-1} cm^{-1}) for 2 min. Each value represents the mean of three independent measurement related to the mass of protein (from Table 2). Dashed bars correspond to the mean of each subset.

275 Despite of a slight heterogeneity in results from the immobilization subsets (I1 to I3), SA of LAC3-MNP hybrids is consistently
276 higher than that of UniK$_{161}$-MNP hybrids and that whatever the nature of the particle. This is consistent with results we
277 have recently obtained on the decolourization of dye models with laccase variants oriented at the surface of silica foams.[39]
278 This trend highlights a general effect exerted by the surface of materials on the oxidation site of the enzyme. Corrected
279 from the bias of initial SA of the free enzymes used for immobilization, the ratio LAC3/UNIK$_{161}$ range from 1.7 to 2.7 (Table
280 3). Related examples of site-directed orientation studies can be found in literature with enzymes as different as lipase,[40]
281 glucose-6-phosphate dehydrogenase,[41] pyrophosphatase,[42] or β-galactosidase.[43] For these enzymes that have structurally
282 defined active sites, the relative loss of enzyme activity (i.e. the ratio of activities of variants with active sites solvent
283 exposed/material exposed) is more or less pronounced, a variation that might be primarily related to the bulkiness of their
284 respective substrates. At the pH of the reaction all three MNPs are negatively charged particles (see SI for zeta potential
285 measurements). Moreover, it is reasonable to think that the negative electrostatic contribution of the enzyme to the overall
286 charge of the surface of the particle can only strengthen this negatively charged surface. This likely provides a repulsive
287 environment for a negatively charged ABTS substrate.[44] On the other hand, in laccase substrate oxidation is an outer sphere
288 mechanism (i.e. there is no coordination of the substrate to the metal) and there is not a truly defined substrate binding
289 site. Therefore, it is tempting to think that the weight of factors like the limitation of diffusion at the liquid/solid interface
290 and steric hindrance may here prevail on that of a deformation of the "active site".

Table 3. Ratios of the specific activity (ABTS) of enzymes grafted on the different MNPs.

	LAC3 / UNIK$_{161}$		
	MNP1	**MNP2**	**MNP3**
Free enzymes[a]	0.8	1.0	1.0
I1	1.7	2.8	1.3
I2	1.2	2.3	3.0
I3	1.7	3.2	1.8
Mean	1.9[a]	2.7	1.7

291
292

[a] SA from 70 to 170 U mg^{-1} depending on batches of enzymes; b corrected from the bias of the initial SA of free enzymes.

293 Given the different spacers we used (scheme 2), the distance from the enzyme surface to the functionalization crown is
294 expected to vary from one grafting to another (calculated to be ≈ 11 to 26 Å, scheme 2). It is generally considered that a
295 short linker conveys more rigidity to the system whereas a longer linker reduces steric hindrance. Comparing SA ratios of
296 the enzymes grafted on MNP1 and MNP2, these constructions seem to comply with this consideration (Table 3). However,
297 it is probable that any "length effect" is here compensated because of the difference of diameter (i.e. $1000 \cdot 10^{-9}$ m for MNP1
298 and $300 \cdot 10^{-9}$ m for MNP2) and therefore of curvature of the particles.[45] On the other hand, despite an enzyme-to-shell
299 distance about 20% longer than for MNP2 as well as a curvature 20 times more pronounced than for MNP1, the SA ratio of
300 LAC3 vs UniK$_{161}$ grafted MNP3 still remains substantially above 1 (Table 3). Therefore, factors tuning the oxidation of the
301 voluminous ABTS include charge and variations of the chemical environment of the oxidation site modulated by the length
302 and the hydrophilic or hydrophobic character of the linker and the nature of the terminal function.

304 **Oxidation of coniferyl alcohol.** Coniferyl alcohol (CA) belongs to the monolignol family of plant secondary metabolites.[46]
305 Compared to ABTS, CA is smaller (8.6 Å vs 17 Å), neutral, hydrophobic. Laccases oxidize coniferyl alcohol generating a
306 resonance stabilized 4-vinylphenoxyl radical (CA$^{\bullet+}$) which dimerises to form the (±) pinoresinol (PINO), (±)
307 dehydrodiconiferyl alcohol (DHCA) and (±) erytro/threo guiacylglycerol (GUA) dimers (scheme SI1). DHCA is the major
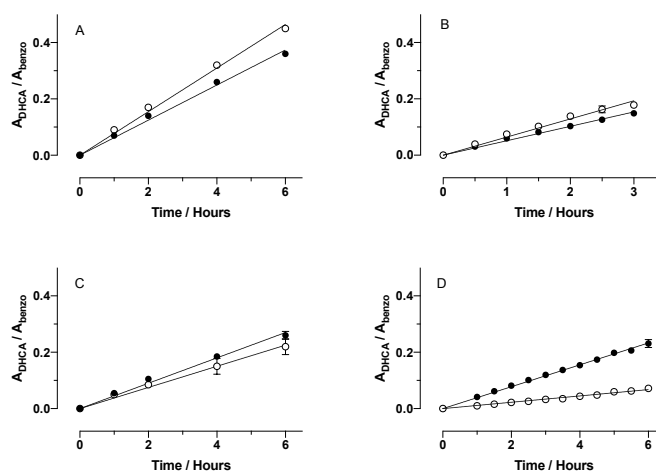308 product amongst the three dimers.

Figure 4: Influence of laccase-MNP hybrids on (±) dehydroconiferyl alcohol (DHCA) production. Laccase-MNPs (accounting for the same final concentration of LAC3 or UniK$_{161}$) incubated at 30°C in 0.1 M acetate buffer pH 5.5 in the presence of coniferyl alcohol (CA, $1.6 \cdot 10^{-3}$ M). The appearance of DHCA (the major CA oxidation product) was followed by HPLC as function of time. Y axis: the peak area of DHCA normalized to the peak area of benzophenone ($1 \cdot 10^{-3}$ M) used as internal standard. A: free enzymes; B: Laccase-MNP3; C: Laccase-MNP1; D: laccase-MNP2. LAC3, closed symbol, UNIK$_{161}$, open symbol. Error bars represent standard deviation on three replicates. Dashed lines are linear regression of data.

309 Substrate consumption and coupling products formation in the presence of the different laccase-MNP hybrids were
310 monitored by HPLC (Fig. SI6). For each experiment, concentrations of LAC3 and UNIK were kept identical and adjusted in
311 order to prevent a rapid exhaustion of the CA substrate. Dimers being oxidizable as well, a low laccase concentration and
312 an excess of CA reduced the bias introduced by concurrent kinetics.[17] In an initial control experiment, with a ratio of slopes
313 LAC3/UNIK$_{161}$ = 0.8, DHCA production appeared slightly faster with free Unik$_{161}$ than with free LAC3 (Fig.4A) and that despite
314 of the use of an identical concentration of enzymes with a similar SA on ABTS (ratio ≈ 1). This small difference may be
315 related to the variation of amino-acid at position 161 since this amino acid is located in an area of the enzyme surface to
316 which phenolic substrates but not ABTS appears to interact with.[34]

317 Laccase-MNP hybrids DHCA production kinetics are presented Figure 4. Amongst the six hybrids tested, the activity of
318 laccase-MNP3 hybrids appears clearly independent of the enzyme orientation. Indeed, using the same amount of LAC3 and
319 Unik$_{161}$ enzymes (as laccase-MNP hybrids) DHCA production proceeds with similar rates (Fig. 4B) with a ratio of slopes
320 LAC3/UNIK$_{161}$ ≈ 1 if one takes into account the bias observed for control homogenous reactions (Fig. 4A). Therefore,
321 contrary to what was previously observed with ABTS for these hybrids, the local microenvironment of the oxidation site
322 has apparently no influence on the oxidation of the small hydrophobic and neutral CA substrate. On the other hand, DHCA
323 production rates are clearly influenced by the orientation of the enzyme at the particle surface and in a differentiated way

324 for the laccase-MNP1 and laccase-MNP2 hybrids (Fig. 4C, D). Indeed, the ratio of slopes LAC3/UNIK$_{161}$ vary from≈ 1.5
325 (laccase-MNP1 hybrids) to > 4 (laccase-MNP2 hybrids). In the absence of the electrostatic effect earlier invoked with ABTS
326 this is a surprisingly marked difference of activity for the UNIK$_{161}$-MNP2 hybrid. As argued before, effects expected from
327 variations of the length of the linker or that of the curvature of the particle are exerted in an opposite way in our
328 constructions. On the other hand, with a small hydrophobic substrate as CA, the hydrophilicity vs hydrophobicity of linkers
329 in MNP1 and MNP2 constructs could be discriminant, which does not seem to be the case in a first analysis. Still, this may
330 apply here while being overwhelmed by the amplitude of another effect, steric for example. Actually, this amplitude may
331 be a consequence of the presence of a benzaldehyde moiety in the grafting linker of the MNP2 particle (Scheme 1). Indeed,
332 resembling a laccase phenolic substrate, it is conceivable that such a free grafting function could increase steric hindrance
333 near the enzyme's oxidation site therefore gating the substrate accessibility. Globally, as studied in laccase-MNP hybrids, it
334 appears that laccase activity can be modulated directly by the functionalization layer. Experiments are ongoing in our
335 laboratories to further investigate on these interfacial effects.

Conclusions

337 We achieved the construction of laccase-(core/shell) magnetic nanoparticles hybrids with different catalytic properties. The
338 precise orientation of the enzyme at the MNPs surface allowed probing the impact of the local environment on laccase
339 activity. Hence, the choice of functionalization layers modulating surface chemical properties of the support to which the
340 oxidation centre located at the surface of enzyme molecules is directly exposed to. With the very same enzyme, we achieve
341 three original interfaces with substantial differences of reactivity the amplitude of which is depending on the nature of the
342 substrate. Beyond consequences expected from varying physical parameters like here the curvature of the particle or the
343 length of the linker, variations of chemical functions in the immediate vicinity of the substrate oxidation appear as a fine
344 tool for the modulation of laccase activity in hybrid biocatalysts. Although immobilization technologies are primarily used
345 for the stabilization and recyclability of enzymes, our results advocate for a careful construction of a structured chemical
346 landscape around the substrate oxidation site. Combined to molecular evolution of the enzyme this should help to design
347 new functions for laccase-hybrid systems.

Conflicts of interest

349 "There are no conflicts to declare".

Acknowledgements

Appendix A. Supplementary data

359 FTIR spectrum of MNP2; TEM images of MNP2; Zeta potentials; Laccase concentration dependency in MNP3 preparations; Elisa tests; Oxidation of
360 coniferyl alcohol; References. See DOI:

References

1   R. A. Sheldon and J. M. Woodley, *Chemical reviews*, 2017, **118**, 801–838.
2   T. Tron in *Encyclopedia of Metalloproteins* (Eds.: R. H. Kretsinger, V. N.Uversky, E. A. Permyakov), Springer, New York, 2013, pp. 1066 –1070.
3   R. A. Abd El Monssef, E. A. Hassan and E. M. Ramadan, *Annals of Agricultural Sciences*, 2016, **61**, 145–154.
4   A. Bronikowski, P.-L. Hagedoorn, K. Koschorreck and V. B. Urlacher, *AMB Express*, 2017, **7**, 73.
5   F. Darvishi, M. Moradi, C. Jolivalt and C. Madzak, *Ecotoxicology and environmental safety*, 2018, **165**, 278–283.
6   C. Ji, J. Hou, K. Wang, Y. H. Ng and V. Chen, *Angew. Chem. Int. Ed.*, 2017, **56**, 9762–9766.
7   J. Sun, N. Guo, L.-L. Niu, Q.-F. Wang, Y.-P. Zang, Y.-G. Zu and Y.-J. Fu, *Molecules*, 2017, **22**, 673.

8   K. Brijwani, A. Rigdon and P. V. Vadlani, *Enzyme Research*, 2010, **2010**, 1–10.

9   M. Ayala, M. A. Pickard and R. Vazquez-Duhalt, *J Mol Microbiol Biotechnol*, 2008, **15**, 172–180.

10   C. J. Rodgers, C. F. Blanford, S. R. Giddens, P. Skamnioti, F. A. Armstrong and S. J. Gurr, *Trends in Biotechnology*, 2010, **28**, 63–72.

11   O. V. Morozova, G. P. Shumakovich, S. V. Shleev and Y. I. Yaropolov, *Applied Biochemistry and Microbiology*, 2007, **43**, 523–535.

12   M. Fernández-Fernández, M. Á. Sanromán and D. Moldes, *Biotechnology Advances*, 2013, **31**, 1808–1825.

13   R. Mehra, J. Muschiol, A. S. Meyer and K.P. Kepp, *Scientific Reports*, 2018, **8**, 1-16.

14   S. Riva. *Trends Biotechnol.*, 2006, 24, 219-26.

15   G. Santiago, F. de Salas, M. F. Lucas, E. Monza, S. Acebes, Á. T. Martinez, S. Camarero and V. Guallar, *ACS Catal.*, 2016, **6**, 5415–5423.

16   M. Fabbrini, C. Galli, P. Gentili and D. Macchitella, *Tetrahedron Letters*, 2001, **42**, 7551–7553.

17   L. Tarrago, C. Modolo, M. Yemloul, V. Robert, P. Rousselot-Pailley and T. Tron, *New Journal of Chemistry*, 2018, **42**, 11770–11775.

18   A. M. Klibanov, *Nature*, 2001, **409**, 241–246.

19   A. Intra, S. Nicotra, S. Riva and B. Danieli, *Advanced Synthesis & Catalysis*, 2005, **347**, 973–977.

20   W. Thiele, S. Obermaier and M. Müller, *ACS Chem. Biol.*, 2020, **15**, 844–848.

21   J. N. Talbert and J. M. Goddard, *Colloids and Surfaces B: Biointerfaces*, 2012, **93**, 8–19.

22   Ievgen Mazurenko, Vivek Pratap Hitaishi, Elisabeth Lojou, *Current Opinion in Electrochemistry*, 2020, **19**, 113-121.

23   C. Mateo, J. M. Palomo, G. Fernandez-Lorente, J. M. Guisan and R. Fernandez-Lafuente, *Enzyme and Microbial Technology*, 2007, **40**, 1451–1463.

24   a) R. G. Chaudhui and S. Paria, *Chem. Rev.*, 2012, 112, 2373-2433; b) R.A. Bohara, N. D. Thorat and S. H. Pawar, *RSC Advances*, 2016, **6**, 43989-44012.

25   O. Barbosa, R. Torres, C. Ortiz, Á. Berenguer-Murcia, R. C. Rodrigues and R. Fernandez-Lafuente, *Biomacromolecules* 2013, **14**, 2433–2462.

26   E. Ahmadi, A. Ramazani, A. Mashhadi-Malekzadeh, Z. Hamdi and Z. Mohamadnia, *Bull. Mater. Sci.* 2014, **37**, 1101-1112.

27   B. Yan and W. Li, *J. Org. Chem*. 1997, **62**, 9354-9357.

28   J. M. McFarland, M. B. Francis, *J. Am. Chem. Soc.* 2005, **127**, 13490-13491.

29   S. Zhou, P. Rousselot-Pailley, L. Ren, Y. Charmasson, E. Courvoisier Dezord, V. Robert, T. Tron and Y. Mekmouche, Methods in Enzymology, 2018, **613**, 17-61.

30   a) N. Lalaoui, P. Rousselot-Pailley, V. Robert, Y. Mekmouche, R. Villalonga, M. Holzinger, S. Cosnier, T. Tron and A. Le Goff, *ACS Catal.*, 2016, **6**, 1894–1900, b) S. Gentil, P. Rousselot-Pailley, F. Sancho, V. Robert, Y. Mekmouche, V. Guallar, T. Tron and A. Le Goff, *Chem. Eur. J.*, 2020, **26**, 4798–4804.

31   a) A. Klonowska, C. Gaudin, A. Fournel, M. Réglier and T. Tron, *Enzyme and Microbial Technology*, 2005, **36**, 34–41; b) Y. Mekmouche, S. Zhou, A. M. Cusano, E. Record, A. Lomascolo, V. Robert, A. J. Simaan, P. Rousselot-Pailley, S. Ullah, F. Chaspoul and T. Tron, *Journal of Bioscience and Bioengineering*, 2014, **117**, 25–27.

32   V. Robert, E. Monza, L. Tarrago, F. Sancho, A. De Falco, L. Schneider, E. Npetgat Ngoutane, Y. Mekmouche, P. R. Pailley, A. J. Simaan, V. Guallar and T. Tron, *ChemPlusChem*, 2017, **82**, 607–614.

33   J. M. McFarland and M. B. Francis, *J. Am. Chem. Soc.*, 2005, **127**, 13490–13491.

34   a) T. Bertrand, C. Jolivalt, P. Briozzo, E. Caminade, N. Joly, C. Madzak and C. Mougin, *Biochemistry*, 2002, **41**, 7325–7333; b) F. J. Enguita, D. Marçal, L. O. Martins, R. Grenha, A. O. Henriques, P. F. Lindley and M. A. Carrondo, *Journal of Biological Chemistry*, 2004, **279**, 23472–23476; c) E. Monza, M. F. Lucas, S. Camarero, L. C. Alejaldre, A. T. Martínez and V. Guallar, *J. Phys. Chem. Lett.*, 2015, **6**, 1447–1453.

35   C. C. S. Fortes, A. L. Daniel-da-Silva, A. M. R. B. Xavier and A. P. M. Tavares, *Chemical Engineering and Processing: Process Intensification*, 2017, **117**, 1–8.

36   a) S. K. S. Patel, V. C. Kalia, J.-H. Choi, J.-R. Haw, I.-W. Kim and J. K. Lee, *Journal of Microbiology and Biotechnology*, 2014, **24**, 639–647; b) H. Wang, W. Zhang, J. Zhao, L. Xu, C. Zhou, L. Chang and L. Wang, *Industrial & Engineering Chemistry Research*, 2013, **52**, 4401–4407; c) S. Rouhani, A. Rostami and A. Salimi, *RSC Adv.*, 2016, **6**, 26709–26718; d) J. N. Vranish, M. G. Ancona, S. A. Walper and I. L. Medintz, *Langmuir*, 2017, **34**, 2901-2925.

37   J. C. Cruz, P. H. Pfromm, J. M. Tomich and M. E. Rezac, *Colloids and Surfaces B: Biointerfaces,* 2010, **79**, 97–104.

38   a) F. Secundo, *Chemical Society Reviews*, 2013, **42**, 6250-6261; b) A. Arsalan and H. Younus, *International journal of biological macromolecules*, 2018, **118**, 1833–1847.

39   F.Yang, R. Backov, J-L. Blin, B. Fáklya, T. Tron, Y. Mekmouche, *Biotechnology Reports*, 2021, **31**, e00645.

40   C. A. Godoy, O. Romero, B. de las Rivas, C. Mateo, G. Fernandez-Lorente, J. M. Guisan, J. M. Palomo, *J. Mol. Cat. B: Enzymatic*, 2013, **87**, 121-127.

41   J. R. Simons, M. Mosisch, A. E. Torda, L. Hilterhaus, *J. Biotechnol.* 2013,**167**,1–7.

42   F. Liu, L. Wang, H. Wang, L. Yuan, J. Li, J. L. Brash, H. Chen, *ACS Appl. Mater. Interfaces,* 2015, **7**, 3717–3724.

43   Y. Li, T. L. Ogorzalek, S. Wei, X. Zhang, P. Yang, J. Jasensky, C. L. Brooks, III, E. Neil G. Marsh, Z. Chen, *Phys. Chem. Chem. Phys.*, 2018, **20**, 1021-1029

44   R. Hong, T. Emrick and V. M. Rotello, *J. Am. Chem. Soc.*, 2004, **126**, 13572–13573.

45   a) A. A. Vertegel, R. W. Siegel, and J. S. Dordick, *Langmuir* 2004, **20**, 6800-6807; b) C. Rodriguez-Quijada, M. Sánchez-Purrà, H. de Puig, and K. Hamad-Schifferli, *J. Phys. Chem. B,* 2018, **122**, 2827–2840.

46   N. G. Lewis and L. B. Davin, in *Comprehensive Natural Products Chemistry*, Elsevier, 1999, pp. 639–712.